

Novel metal-chelate affinity sorbents for reversible use in catalase adsorption

Sinan Akgöl, Adil Denizli*

Department of Chemistry, Hacettepe University, P.K. 51, Sımanpazar, Ankara 06242, Turkey

Received 10 July 2003; received in revised form 5 December 2003; accepted 22 December 2003

Abstract

A novel metal-chelate adsorbent utilizing *N*-methacryloyl-(*L*)-histidine methyl ester (MAH) as a metal-chelating ligand was prepared. MAH was synthesized by using methacryloyl chloride and *L*-histidine methyl ester dihydrochloride. Magnetic beads with an average size of 150–250 μm were obtained by suspension polymerization of ethylene glycol dimethacrylate (EGDMA), and MAH conducted in aqueous dispersion medium. The specific surface area of the porous beads was found to be 80.1 m^2/g . Mag-poly(EGDMA–MAH) beads were characterized by swelling tests, electron spin resonance (ESR), nuclear magnetic resonance (NMR) and scanning electron microscopy (SEM). Elemental analysis of MAH for nitrogen was estimated as 43.9 $\mu\text{mol}/\text{g}$. Then, Fe^{3+} ions were chelated on the magnetic beads. Fe^{3+} -chelated magnetic beads with a swelling ratio of 40% were used in the adsorption of catalase in batch system. The maximum catalase adsorption capacity of the mag-poly(EGDMA–MAH)– Fe^{3+} beads was observed as 83.2 mg/g at pH 7.0. The K_m values for immobilized catalase (mag-poly(EGDMA–MAH)– Fe^{3+}) (20.5 mM) were higher than that of free enzyme (16.5 mM). Storage stability was found to increase with immobilization. It was observed that enzyme could be repeatedly adsorbed and desorbed without significant loss in adsorption capacity or enzyme activity.

© 2004 Elsevier B.V. All rights reserved.

Keywords: Enzyme immobilization; IMAC; Histidine; Affinity beads; Catalase; Magnetic support

1. Introduction

Immobilized metal ion affinity chromatography (IMAC) has become a widespread analytical and preparative separation method for therapeutic proteins, peptides, nucleic acids, hormones, and enzymes [1–5]. Many transition metals can form stable complexes with electron-rich compounds and may coordinate molecules containing O, N and S by ion-dipole interactions. Metal ions and ligands are first-row transition metals (Zn^{2+} , Ni^{2+} , Cu^{2+} , and Fe^{3+}) in combination with iminodiacetic acid, nitrilotriacetic acid, tris(carboxymethyl)ethylene-diamine. IMAC introduces a new approach for selectively interacting materials on the basis of their affinities for chelated metal ions. The separation is based on the interaction of a Lewis acid (electron pair donor), i.e. a chelated metal ion, with an electron acceptor group on the surface of the protein [6–8]. Proteins are as-

sumed to interact mainly through the imidazole group of histidine and, to a lesser extent, the indoyl group of tryptophan and the thiol group of cysteine. Co-operation between neighboring amino acid side chains and local conformations plays an important role in protein binding. Aromatic amino acids and the amino-terminus of the peptides also have some contributions [9]. The low cost of metals and the reuse of adsorbents for hundreds of times without any detectable loss of metal-chelating properties are the attractive features of metal affinity separation.

The development of the magnetic adsorbents promises to solve many of the problems associated with chromatographic separations in packed bed and in conventional fluidized bed systems [10]. Magnetic adsorbents combine some of the best characteristics of fluidized beds (low pressure drop and high feed-stream solid tolerances) and of fixed beds (absence of particle mixing, high mass transfer rates, and good fluid–solid contact) [11]. Recently, there has been increased interest in the use of magnetic adsorbents in protein purification [12]. Magnetic adsorbents can be produced using inorganic materials or a number of synthetic

* Corresponding author.

E-mail address: denizli@hacettepe.edu.tr (A. Denizli).

and natural polymers. High mechanical resistance, insolubility and excellent shelf life make inorganic materials ideal as carriers. The main disadvantage of inorganic adsorbents is their limited functional groups for chelation with metal ions. Magnetic adsorbents can be porous or non-porous [13]. Magnetic adsorbents are more commonly manufactured from polymers since they have a variety of surface functional groups which can be tailored for use in different applications [14–19].

Catalase is a heme containing metalloenzyme and regarded as one of the most common enzymes in plant and animal tissues and has a protection function connected with the decomposition of hydrogen peroxide [20]. Catalase consists of four subunits, each of them involving ferriporphyrin as a prosthetic group. Immobilized catalase has useful applications in the food industry in the removal of hydrogen peroxide from food products after cold pasteurization, and in the analytical field, as a component of hydrogen peroxide and glucose-biosensor systems [21–26].

In this study, we propose *N*-methacryloyl-(*L*)-histidine methyl ester (MAH) as a new metal-chelating ligand and/or comonomer for use in the IMAC for catalase. MAH was synthesized from methacryloyl chloride and *L*-histidine methyl ester. Magnetic poly(ethylene glycol dimethacrylate-*N*-methacryloyl-(*L*)-histidine methyl ester) [poly(EGDMA–MAH)] beads were produced by suspension polymerization of MAH and ethylene glycol dimethacrylate (EGDMA) in the presence of magnetite. Then, Fe^{3+} ions were chelated on these magnetic beads. Poly(EGDMA–MAH) magnetic beads were characterized by NMR, ESR, FTIR, SEM, and elemental analysis. Then, bovine liver catalase was adsorbed on the metal-chelating beads from aqueous solutions containing different amounts of catalase, at different pH's. Desorption of catalase and reusability of these metal-chelate affinity adsorbents were also tested.

2. Materials and methods

2.1. Materials

Bovine liver catalase (hydrogen peroxide oxidoreductase, E.C. 1.11.1.6), *L*-histidine methyl ester, methacryloyl chloride were supplied by Sigma (St Louis, USA). EGDMA was obtained from Fluka A.G (Buchs, Switzerland), distilled under reduced pressure in the presence of hydroquinone inhibitor and stored at 4 °C until use. Benzoyl peroxide (BPO) was obtained from Fluka. Poly(vinyl alcohol) (PVAL; MW:100.000, 98% hydrolyzed) was supplied from Aldrich (USA). All other chemicals were of reagent grade and were purchased from Merck A.G. (Darmstadt, Germany). All water used in the experiments was purified using a Barnstead (Dubuque, IA) ROPure LP[®] reverse osmosis unit with a high flow cellulose acetate membrane (Barnstead D2731) followed by a Barnstead 3804 NANOPURE[®] organic/colloid removal and ion-exchange packed-bed system.

2.2. Synthesis of MAH

For the synthesis of MAH, the following experimental procedure was applied; 5.0 g of *L*-histidine methylester and 0.2 g of hydroquinone were dissolved in 100 ml of dichloromethane solution. This solution was cooled down to 0 °C and 12.7 g of triethylamine was added to the solution. Five milliliter of methacryloyl chloride was poured slowly into this solution which was stirred magnetically at room temperature for 2 h. At the end of the chemical reaction period, hydroquinone and unreacted methacryloyl chloride were extracted with 10% NaOH solution. The aqueous phase was evaporated in a rotary evaporator. The residue (i.e. MAH) was crystallized in an ether–cyclohexane mixture and then dissolved in ethyl alcohol.

2.3. Preparation of magnetic poly(EGDMA–MAH) beads

Magnetic poly(EGDMA–MAH) beads were prepared by a suspension polymerization. A typical procedure may be summarized as follows: The stabilizer, PVAL, was dissolved in 50 ml deionized water for the preparation of the continuous phase. The dispersion phase was prepared by mixing EGDMA (8.0 ml), MAH (1.0 g) and toluene (12.0 ml) in a test tube. The initiator, BPO (100 mg), was dissolved in this homogeneous solution. The dispersion phase was added to the continuous medium in a glass-sealed polymerization reactor (100 ml) placed in a water bath equipped with a temperature-control system. The polymerization reactor was heated to 65 °C within about 30 min by stirring the polymerization medium at 600 rpm. The polymerization was conducted at 65 °C for 4 h and at 90 °C for 2 h. After completion of polymerization, the reactor content was cooled to room temperature. A washing procedure was applied after polymerization to remove the diluent and any possible unreacted monomers and other ingredients from the beads. The magnetic beads were filtered and resuspended in ethyl alcohol. The suspension was stirred for about 1 h at room temperature and the beads were separated by filtration. The beads were washed twice with ethyl alcohol and then four times with deionized water using the same procedure. When not in use, the beads were kept under refrigeration in 0.02% sodium azide solution to prevent microbial contamination.

2.4. Characterization of the magnetic beads

The specific surface area of the beads was determined in a BET apparatus (Micrometrics ASAP 2000 Sorptometer, USA). The average size and size distribution of the beads were determined by screen analysis performed using Tyler Standard Sieves.

Water-uptake ratios of the beads were determined in distilled water. The experiment was conducted as follows: initially dry beads were carefully weighed before being placed in a 50 ml vial containing distilled water. The vial was put into an isothermal water bath with a fixed temperature

($25 \pm 0.5^\circ\text{C}$) for 2 h. The beads were taken out from the water, wiped using a filter paper, and weighed. The weight ratio of dry and wet samples was recorded. The water content of the beads was calculated using the following expression:

$$\text{Water-uptake ratio (\%)} = \left[\frac{W_s \pm W_o}{W_o} \right] \times 100 \quad (1)$$

W_o and W_s are the weights of beads before and after uptake of water, respectively.

The surface morphology of the magnetic beads was examined using SEM. The samples were initially dried in air at 25°C for 7 days before being analyzed. A fragment of the dried bead was mounted on a SEM sample mount and was sputter coated for 2 min. The sample was then mounted in a scanning electron microscope (Model: JEOL Model JMS-5600, Japan). The surface of the sample was then scanned at the desired magnification to study the morphology of the beads.

To evaluate the degree of MAH incorporation the synthesized mag-poly(EGDMA–MAH) beads were subjected to elemental analysis using a Leco Elemental Analyzer (Model CHNS-932).

The ^1H NMR spectrum of MAH monomer was taken in CDCl_3 on a JEOL GX-400 300 MHz instrument. The residual non-deuterated solvent (CHCl_3) served as an internal reference. Chemical shifts are reported in parts per million (δ) downfield relative to CHCl_3 .

The degree of magnetism of the poly(EGDMA–MAH) beads was measured in a magnetic field by using a vibrating-sample magnetometer (Princeton Applied Research, Model 150A, USA). The presence of magnetite particles in the polymeric structure was investigated with an electron spin resonance (ESR) spectrophotometer (EL 9, Varian).

2.5. Incorporation of Fe^{3+} Ions

Chelates of Fe^{3+} ions with mag-poly(EGDMA–MAH) beads were prepared as follows: 1.0 g of the magnetic beads were mixed with 50 ml of aqueous solutions containing 30 ppm Fe^{3+} ions, at constant pH of 5.0 (adjusted with HCl and NaOH), which was the optimum pH for Fe^{3+} chelate formation at room temperature. A 1000 ppm atomic absorption standard solution (containing 10% HNO_3) was used as the source of Fe^{3+} ions. The flask was stirred magnetically at 100 rpm for 1 h (sufficient to reach equilibrium). The concentration of the Fe^{3+} ions in the resulting solution was determined with a graphite furnace atomic absorption spectrometer (AA800, Perkin Elmer, Bodenseewerk, Germany). The Fe^{3+} chelation step is depicted in Fig. 1. The amount of adsorbed Fe^{3+} ions was calculated by using the concentrations of the Fe^{3+} ions in the initial solution and in the equilibrium.

Fe^{3+} leakage from the poly(EGDMA–MAH) beads was investigated with media pH (6.0–8.0), and also in a medium containing 1.0 M NaSCN. The magnetic bead suspensions were stirred 24 h at room temperature. Fe^{3+} ion concentra-

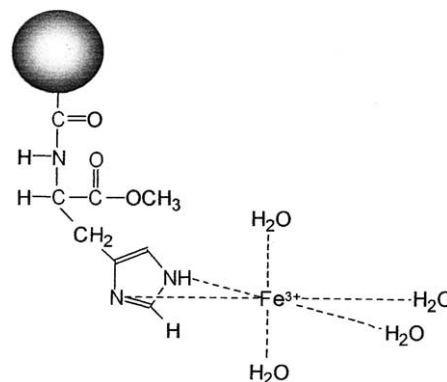


Fig. 1. Schematic diagram for the chelation of Fe^{3+} ions through the magnetic beads.

tion was then determined in the supernatants using an atomic absorption spectrophotometer. It should be also noted that immobilized metal containing beads were stored at 4°C in the 10 mM Tris–HCl buffer (pH 7.4) with 0.02% sodium azide to prevent microbial contamination.

2.6. Catalase adsorption studies

Catalase adsorption by the Fe^{3+} -chelated mag-poly(EGDMA–MAH) beads was studied at various pH values, either in acetate buffer (0.1 M, pH 4.0–5.5) or in phosphate buffer (0.1 M, pH 6.0–8.0). Initial catalase concentration was 1.0 mg/ml in the corresponding buffer. The adsorption experiments were conducted for 2 h at 25°C while stirring continuously. At the end of this period, the enzyme adsorbed beads was removed from the enzyme solution and was washed with the same buffer three times. It was stored at 4°C in fresh buffer until use. The amount of adsorbed catalase was calculated as:

$$Q = \frac{[(C_o - C) V]}{m} \quad (2)$$

Here, Q is the amount of catalase adsorbed onto unit mass of beads (mg/g); C_o and C are the concentrations of catalase in the initial solution and in the aqueous phase after treatment for certain period of time, respectively (mg/ml); V is the volume of the aqueous phase (ml); and m is the mass of the beads used (g).

In order to determine the adsorption capacities of mag-poly(EGDMA–MAH)– Fe^{3+} beads, the concentration of catalase in the medium was varied in the range 0.05–1.0 mg/ml.

2.7. Desorption of catalase from Fe^{3+} -chelated beads

In order to determine the reusability of the mag-poly(EGDMA–MAH)– Fe^{3+} beads, the catalase adsorption and desorption cycle was repeated five times. The catalase desorption from mag-poly(EGDMA–MAH)– Fe^{3+} beads was carried out with 1.0 M NaSCN solution at pH 8.0. The beads

were washed several times with phosphate buffer (0.1 M, pH 7.0), and were then reused in enzyme immobilization.

2.8. Determination of immobilization efficiency

The amount of protein in the crystalline-enzyme preparation and in the wash solution was determined by spectrofluorimetry (excitation 280 nm and emission 340 nm) using a Shimadzu (Model RF 5301-PC) spectrofluorimeter.

2.9. Activity assays of free and immobilized catalase

Catalase activity was determined spectrophotometrically by direct measurement of the decrease in the absorbance of hydrogen peroxide at 240 nm, due to its decomposition by the enzyme. Hydrogen peroxide solutions (5–30 mM) were used to determine the activity of both the free and immobilized enzymes. A 4 ml portion of the reaction mixture was pre-incubated at 25 °C for 10 min and the reaction was started by adding 50 μ l of catalase solution (100 μ g/ml). The decrease in absorbance at 240 nm was recorded for 5 min. The rate of change in the absorbance (Δ_{240}/min) was calculated from the initial linear portion, with the use of the calibration curve (absorbance of hydrogen peroxide solutions of various concentration (5–30 mM) at 240 nm). One unit of activity is defined as the decomposition of 1 μ mol/min of hydrogen peroxide at 25 °C and pH 7.0. These activity assays were carried out over the pH range 4.0–8.0 and temperature range 5–60 °C to determine the pH and temperature profiles for the free and the immobilized enzymes. The effect of substrate concentration was tested in the 5–30 mM hydrogen peroxide range. The results of pH, temperature and substrate concentration of the medium are presented in a normalized form, with the highest value of each set being assigned the value for 100% activity.

2.10. Storage stability

The activity of free and adsorbed catalase in phosphate buffer (0.1 M, pH 7.0) was measured in a batch-operation mode at 4 °C.

3. Results and discussion

3.1. Characterization of beads

The poly(EGDMA) and mag-poly(EGDMA–MAH) beads are crosslinked gels. They do not dissolve in aqueous medium, but do swell, depending on the degree of cross-linking. The equilibrium swelling ratio of the mag-poly(EGDMA–MAH) beads is 40%. Compared with poly(EGDMA) (17.7%), the water uptake ratio of the mag-poly(EGDMA–MAH) beads was increased. Several possible factors may contribute to this result. First, the in-

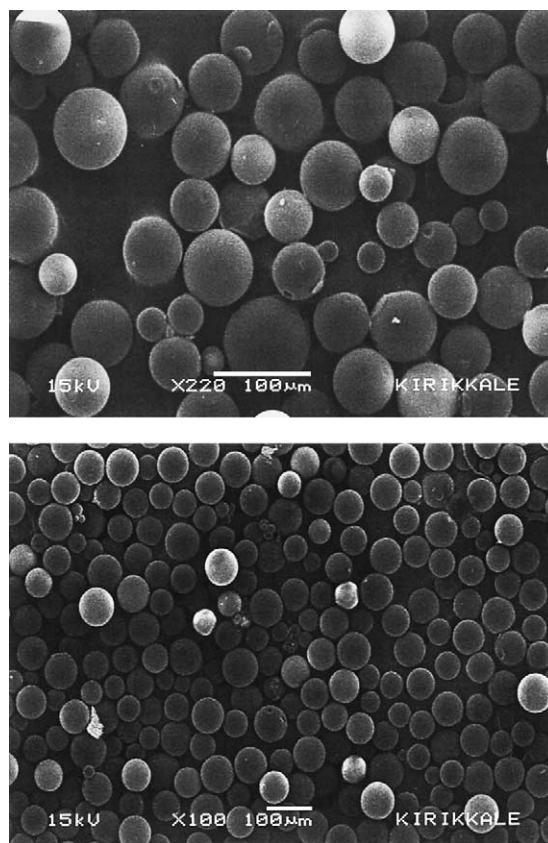


Fig. 2. SEM micrographs of mag-poly(EGDMA–MAH) beads.

corporation of MAH actually introduces more hydrophilic functional groups into the polymer chain, which can attract more water molecules into polymer matrices. Second, the reaction of MAH with EGDMA could effectively decrease the molecular weight of the resulting polymer. Therefore, the water molecules penetrate into the entangled polymer chains more easily, resulting in an improvement of water uptake behavior in aqueous solutions.

The surface morphologies of mag-poly(EGDMA–MAH) beads are exemplified by the electron micrographs in Fig. 2. As is clearly seen here, the beads have a spherical form and a rough surface due to the pores which formed during the polymerization procedure. The presence of pores within the bead surface is clearly seen in this photograph. It can be concluded that the mag-poly(EGDMA–MAH) beads have a porous interior surrounded by a reasonably rough surface, in the dry state. The roughness of the surface should be considered as a factor providing an increase in the surface area. In addition, these pores reduce diffusional resistance and facilitate mass transfer because of high internal surface area.

To evaluate the degree of MAH incorporation into the polymeric structure, elemental analysis of the synthesized mag-poly(EGDMA–MAH) beads was performed. The incorporation of the MAH was found to be 43.9 μ mol/g polymer using nitrogen stoichiometry.

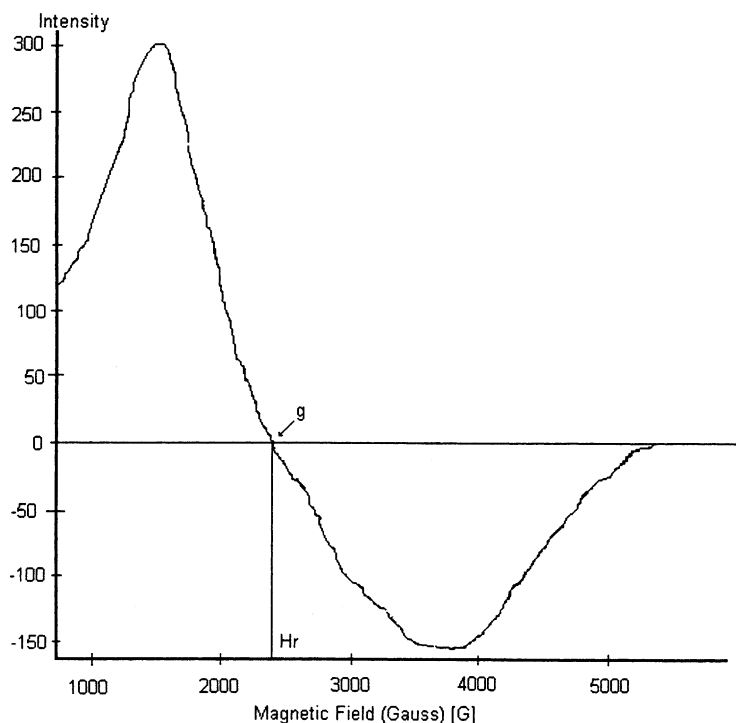


Fig. 3. The magnetic behavior of mag-poly(EGDMA–MAH) beads.

Maximum Fe^{+3} loading was found to be $6.4 \mu\text{mol/g}$ polymer.

The radical suspension polymerization procedure provided crosslinked mag-poly(EGDMA–MAH) beads in a spherical form mostly in the size range of $150\text{--}250 \mu\text{m}$. The specific surface area of the mag-poly(EGDMA–MAH) beads was found to be $81 \text{ m}^2/\text{g}$.

^1H NMR spectroscopy was used to determine the structure of MAH. Characteristic peaks are as follows: ^1H NMR (CDCl_3): $\delta = 1.99$ (*t*; 3H, $J = 7.08 \text{ Hz}$, CH_3), 1.42 (*m*; 2H, CH_2), 3.56 (*t*; 3H, O-CH_3), $4.82\text{--}4.87$ (*m*; 1H, methin), 5.26 (*s*; 1H, vinyl H), 5.58 (*s*; 1H, vinyl); 6.86 (δ ; 1H, $J = 7.4 \text{ Hz}$, NH), 7.82 (δ ; 1H, $J = 8.4 \text{ Hz}$, NH), $6.86\text{--}7.52$ (*m*; 5H, aromatic).

The presence of magnetite particles in the polymeric structure was confirmed by ESR. The intensity of the magnetite peak against magnetic field (Gauss) is shown in Fig. 3.

The application of an external magnetic field may generate an internal magnetic field in the sample which will either be added or subtracted from the external field. The local magnetic field generated by the electronic magnetic moment will add vectorially to the external magnetic field (H_{ext}) to give an effective field (H_{eff}).

$$H_{\text{eff}} = H_{\text{ext}} + H_{\text{local}} \quad (3)$$

As seen in Fig. 3, mag-poly(EGDMA–MAH) beads have a relative intensity of 125. This value shows that the polymeric structure has a local magnetic field because of magnetite in its structure. The g factor given in Fig. 3 can be considered as being characteristic of the molecules in which the unpaired

electrons are located, and it is calculated from Eq. (3). The measurement of the g factor for an unknown signal can be a valuable aid in the identification of a signal's origin. In the literature the g factor for Fe^{+3} (low spin and high spin complexes) is determined between $1.4\text{--}3.1$ and $2.0\text{--}9.7$, respectively [27]. The g factor was found to be 2.56 for mag-poly(EGDMA–MAH) beads.

3.2. Adsorption efficiency and retention of activity

The effect of pH on the adsorption of catalase onto mag-poly(EGDMA–MAH)– Fe^{+3} beads was studied in the pH range $4.0\text{--}8.0$ and the effects of pH on adsorption are presented in Fig. 4. The decrease in the protein adsorption capacity in more acidic and more alkaline regions can be attributed to electrostatic repulsion effects between the opposite charged groups. Proteins have no net charge at their isoelectric points, and therefore the maximum adsorption from aqueous solutions is usually observed at their isoelectric points. The isoelectric pH of catalase is 6.35. In the present study, the maximum adsorption was not at this pH, but had slightly shifted toward more neutral pH values. This could be due to preferential interactions between catalase molecules and Fe^{+3} incorporated polymeric matrix at neutral pH.

The adsorption isotherm of catalase is presented for Fe^{+3} -chelated mag-poly(EGDMA–MAH) beads in Fig. 5. An increase in catalase concentration in the adsorption medium led to an increase in adsorption efficiency but this levelled off at catalase concentration of 0.3 mg/ml . Maximum catalase adsorption was obtained for mag-poly(EGDMA–MAH)– Fe^{+3} beads (83.2 mg/g). This

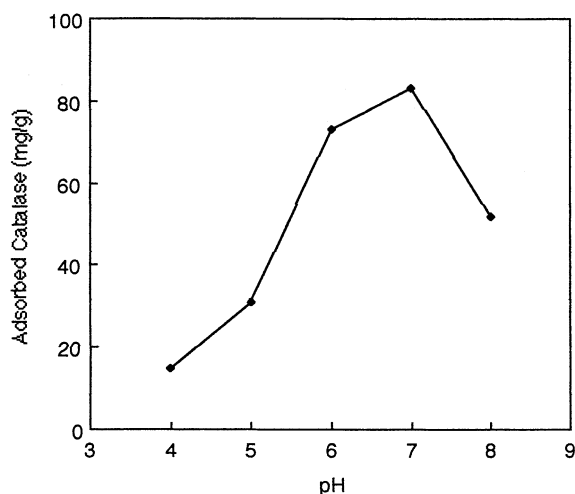


Fig. 4. Effect of pH on catalase adsorption onto mag-poly(EGDMA-MAH)-Fe³⁺ beads.

could be due to the specific interactions between catalase and chelated-Fe³⁺ ions, because catalase has an iron protoporphyrin prosthetic group.

Kinetic parameters, Michaelis constants K_m and V_{max} for free and immobilized catalase were determined using Lineweaver-Burk plot. Hydrogen peroxide was used as the substrate. For the free enzyme, K_m was found to be 16.5 mM, whereas V_{max} was calculated as 236×10^3 U/mg protein.

Kinetic constants of the immobilized catalase were also determined in a batch system. K_m values were found to be 20.5 mM for mag-poly(EGDMA-MAH)-Fe³⁺-catalase preparation. The V_{max} values of immobilized enzyme for mag-poly(EGDMA-MAH)-Fe³⁺-catalase preparation were estimated from the data as 220×10^3 U/mg of adsorbed protein onto mag-poly(EGDMA-MAH) beads. As expected, the K_m and V_{max} values were significantly affected after adsorption onto the Fe³⁺ incorporated mag-poly(EGDMA-MAH) beads.

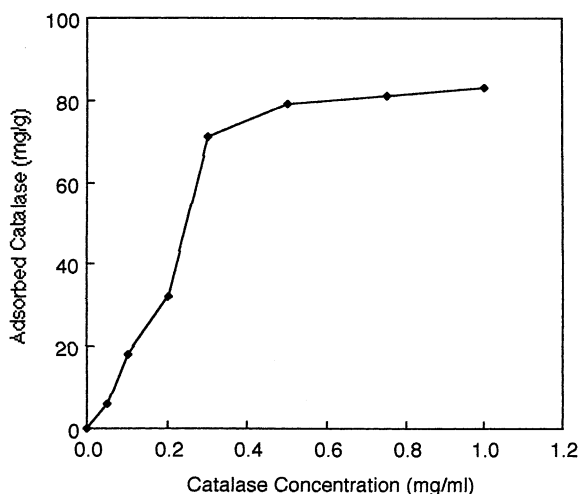


Fig. 5. Effect of catalase concentration on the adsorption efficiency of mag-poly(EGDMA-MAH)-Fe³⁺ beads.

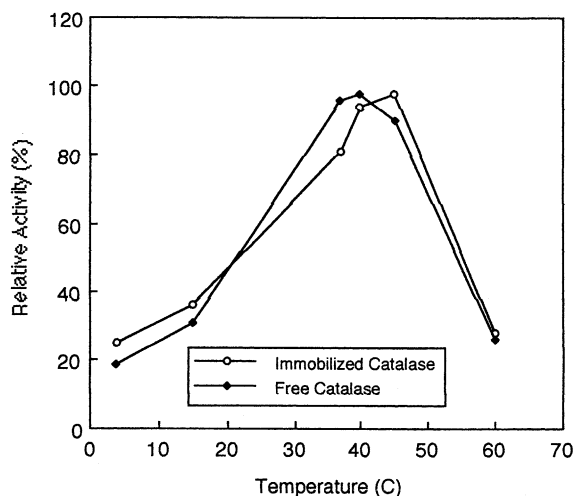


Fig. 6. Temperature profiles of free and adsorbed catalase.

3.3. Effect of temperature on the catalytic activity

In general, the effects of changes in temperature on the rates of enzyme-catalyzed reactions do not provide much information on the mechanism of catalysis. However, these effects could be important in indicating structural changes in enzymes [28]. In Fig. 6, the relative activities of both the free and the immobilized catalase as a function of temperature are reported, together with that of the free enzyme for comparison. The optimum temperature for the immobilized preparation of mag-poly(EGDMA-MAH)-Fe³⁺-Catalase at 45 °C, 5 °C higher than that of the free enzyme at 40 °C.

3.4. Effect of pH on the activity

The pH effect on the activity of the free and immobilized catalase preparations for hydrogen peroxide degradation was studied. The effect of pH on the free and the immobilized preparations was investigated in the pH range between 4.0 and 8.0 in acetate and phosphate buffers and the results are presented in Fig. 7. The data show that mag-poly(EGDMA-MAH)-Fe³⁺-catalase preparation has the same optimum as the free enzyme (pH: 7.0). The immobilized preparations gave a significantly broader profile than that of the free enzyme. It was between 6.5 and 7.0. The pH profiles of the immobilized enzymes were much broader with respect to the free enzyme, probably due to the production of oxygen, forming bubbles, and causing external diffusional limitations on the enzyme-polymer beads surface.

3.5. Storage stability

Free and immobilized catalase preparations were stored in a phosphate buffer (0.1 M, pH 7.0) at 4 °C and the activity measurements were carried out for a period of 50 days (Fig. 8). No enzyme release was observed. The free enzyme

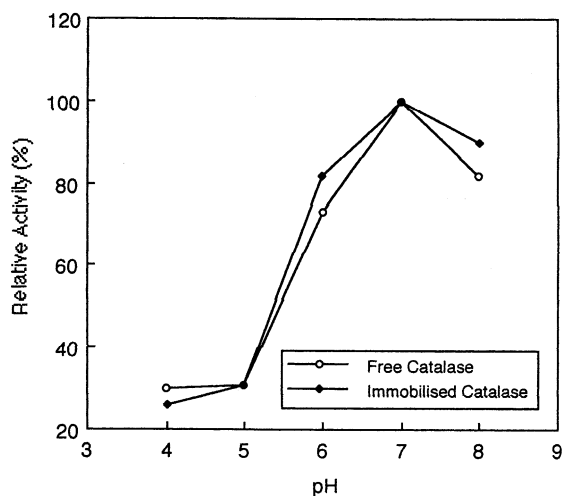


Fig. 7. pH profiles of free and adsorbed catalase.

lost all of its activity within 18 days. Immobilized preparation of mag-poly(EGDMA–MAH)–Fe⁺³-Catalase lost 20% of its activity during the same period. This decrease in enzyme activity was explained as a time-dependent natural loss in enzyme activity and this was prevented to a significant degree upon immobilization.

3.6. Repeated use

Desorptions of catalase from Fe⁺³-chelated mag-poly(EGDMA–MAH) beads were carried out in a batch system. Mag-poly(EGDMA–MAH)–Fe⁺³-catalase preparation was placed within the desorption medium containing 0.1 M NaSCN (pH 8.0) at room temperature for 2 h. It was then repeatedly used in adsorption of catalase. The catalase adsorption capacity was not change during the five successive adsorption–desorption (Fig. 9). Enzyme activities of preparations did not significantly change during these adsorption–desorption cycles. These results showed

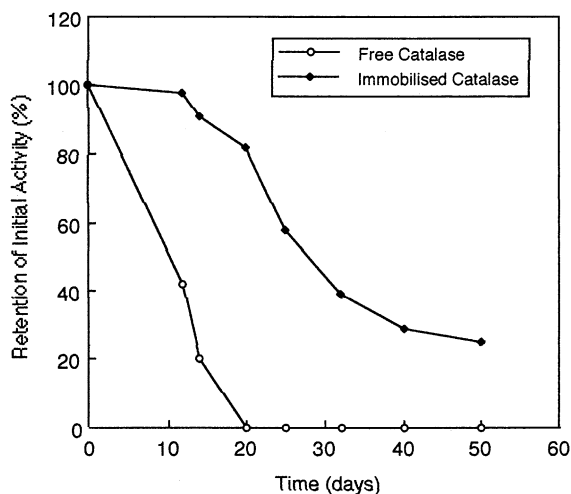


Fig. 8. Storage stability of adsorbed catalase.

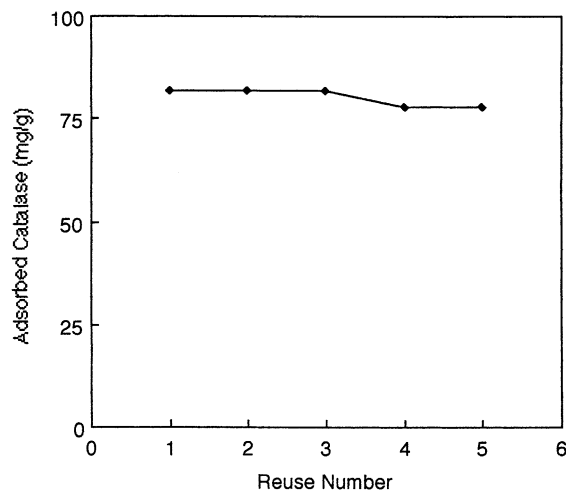


Fig. 9. Repeated used of Fe⁺³ incorporated mag-poly(EGDMA–MAH) beads.

that Fe⁺³ incorporated, novel mag-poly(EGDMA–MAH) beads can be repeatedly used in enzyme immobilization, without detectable losses in their initial adsorption capacities.

4. Conclusions

The time consuming and high cost of metal-chelating procedure has inspired a search for suitable low-cost adsorbents. The main advantage of IMAC consists in its simplicity, universality, stability and cheapness of the chelating supports [29–31]. In addition, the IMAC supports ensure the milder elution conditions of proteins, retaining their biological activity. In this study, a novel *N*-methacryloyl-(L)-histidine methyl ester (MAH)-containing magnetic affinity adsorbent for the separation of catalase was prepared. This new approach for the preparation of metal-chelating adsorbent has many advantages over conventional techniques. An expensive and critical step in the preparation process of metal-chelating adsorbent is coupling of a chelating ligand to the adsorption matrix. In this procedure, comonomer MAH acted as the metal-chelating ligand, and there is no need to activate the matrix for the chelating-ligand immobilization. Another major issue is that of slow release of these covalently bonded chelators from the matrix. Metal-chelating ligand release is a general problem encountered in any immobilized metal-chelate affinity adsorption technique which causes a decrease in adsorption capacity. It is well known that metal-chelating ligand leakage from the adsorbent causes contaminations that will interfere with analysis of the purified protein. Metal-chelating ligand immobilization step was also eliminated in this approach. Metal-chelating ligand and/or comonomer MAH was polymerized with HEMA and there is no leakage of the ligand. This purification method will overcome the drawback of multi-step purification methods.

Acknowledgements

The authors wish to express their thanks to Dr. M.Y. Arica for his help in the taking of SEM photographs.

References

- [1] M.N. Gupta, S. Jain, I. Roy, *Biotechnol. Prog.* 18 (2002) 78.
- [2] G. Tishchenko, J. Dybal, J.K. Meszarova, Z. Sedlakova, M. Bleha, *J. Chromatogr. A.* 954 (2002) 115.
- [3] M.Y. Arica, H.N. Testereci, A. Denizli, *J. Chromatogr. A.* 799 (1998) 83.
- [4] F. Denizli, A. Denizli, M.Y. Arica, *Polym. Int.* 48 (1999) 360.
- [5] V. Gaberc-Porekar, V. Menart, *J. Biochem. Biophys. Meth.* 49 (2001) 335.
- [6] G.S. Chaga, *J. Biochem. Biophys. Meth.* 49 (2001) 313.
- [7] A. Denizli, F. Denizli, E. Piskin, *J. Biomater. Sci., Polym. Ed.* 10 (1999) 305.
- [8] C.Y. Wu, S.Y. Suen, S.C. Chen, J.H. Tzeng, *J. Chromatogr. A.* 996 (2003) 53.
- [9] T.T. Yip, T.W. Hutchens, *Mol. Biotechnol.* 1 (1994) 151.
- [10] C.J. Fee, *AIChEJ* 42 (1996) 1213.
- [11] D.J. Graves, *Chromatogr. Sci.* 61 (1993) 187.
- [12] T. Hultman, S. Stahl, E. Hornes, M. Uhlen, *Nucleic Acids Res.* 17 (1989) 4937.
- [13] P.J. Halling, M.D. Dunhill, *Enzyme Microbial Technol.* 2 (1980) 136.
- [14] A. Denizli, *J. Chromatogr. A.* 793 (1998) 47.
- [15] B.A. Balto, *J. Macromol. Sci. Chem. A* 14 (1980) 107.
- [16] T.M. Cocker, C.J. Fee, R.A. Evans, *Biotechnol. Bioeng.* 53 (1997) 79.
- [17] A.S. Chetty, M.A. Burns, *Biotechnol. Bioeng.* 38 (1991) 963.
- [18] M.Y. Arica, H. Yavuz, S. Patr, A. Denizli, *J. Mol. Catal. B: Enzymatic* 11 (2000) 127.
- [19] M. Odabasi, A. Denizli, *J. Chromatogr. B.* 760 (2001) 137.
- [20] S. Akgöl, A. Denizli, M.Y. Arica, *Food Chem.* 74 (2001) 281.
- [21] E. Horozova, N. Dimcheva, Z. Jordanova, *Bioelectrochem.* 53 (2000) 11.
- [22] M. Dixon, E. Well, *Enzymes*, Longman, Gren and Company, London, 1964.
- [23] L. Tarhan, *Biomed. Biochem. Acta* 49 (1990) 307.
- [24] P.T. Vasudevan, D.S. Thakur, *Appl. Biochem. Biotechnol.* 49 (1995) 173.
- [25] S. Akgol, E. Dincaya, *Talanta* 48 (1999) 363.
- [26] M.Y. Arica, A. Denizli, E. Piskin, V. Hasrc, *J. Membr. Sci.* 129 (1997) 65.
- [27] H.M. Swartz, J.R. Bolton, D.C. Borg, Wiley, New York, 1972, 1997, p. 1843.
- [28] M.M. El-Masry, A. De Maio, S. Di Martino, N. Diano, U. Ben-civenga, S. Rossi, V. Grano, P. Canciglia, M. Portaccio, F.S. Gaeta, D.G. Mita, *J. Mol. Catal. B.* 9 (2000) 219.
- [29] E.K.M. Ueda, P.W. Gout, L. Morganti, *J. Chromatogr. A.* 988 (2003) 1.
- [30] A. Denizli, E. Piskin, *J. Chromatogr. A.* 731 (1996) 57.
- [31] S. Emir, R. Say, H. Yavuz, A. Denizli, *Biotechnol. Prog.* 2004, in press.